Global CKM Fits with the Scan Method

Gerald Eigen,[*][†]
University of Bergen
E-mail: gerald.eigen@ift.uib.no

Gregory Dubois-Felsmann
SLAC
E-mail: gpdf@slac.stanford.edu

David G. Hitlin, Frank C. Porter
Caltech
E-mail: hitlin@caltech.edu, fcp@caltech.edu

We present results of unitary triangle fits based on the scan method. This frequentist approach uses Gaussian uncertainties for experimental quantities, but makes no arbitrary assumptions about the distribution of theoretical errors. Instead, we perform a large number of fits, scanning over regions of plausible theory uncertainties for each quantity, and retain those fits meeting a specific confidence level criterion, thereby constraining the $\bar{\rho} - \bar{\eta}$ plane using the standard input measurements (CKM matrix elements, $\sin 2\beta$, $B_{d,s}^0$ mixing, ε_K) as well as branching fraction and *CP* asymmetry measurements of *B* decays to $B \to PP, PV, VV$ and $a_1 P$ decay modes to determine α, $D^{(*)}K^{(*)}$ modes to determine γ, and $D^{(*)}\pi$ and $D\rho$ modes to determine $2\beta + \gamma$. We parameterize individual decay amplitudes in terms of color-allowed tree, color-suppressed tree, penguin, singlet penguin, electroweak penguin, color-suppressed electroweak as well as *W*-exchange and *W*-annihilation amplitudes. With this parameterization, we obtain a good fit to the measured branching fractions and *CP* asymmetries with no new physics contributions. This simultaneous fit allows us to determine the correlation between α and β.

---

[*]Speaker.

1. Introduction

The phase of the Cabibbo-Kobayashi-Maskawa (CKM) matrix [1] produces *CP* violation in the Standard Model (SM). Unitarity relations provide an excellent laboratory to test this prediction. The relation $V_{ub}^* V_{ud} + V_{cb}^* V_{cd} + V_{tb}^* V_{td} = 0$ is particularly useful, since many measurements in the *B* and *K* systems can be combined for this test.

2. Fit Methodology

The scan method is a frequentist-based fitting technique of the CKM matrix [2]. It accounts for theory uncertainties in the QCD parameters $f_{B_s}, f_{B_s}/f_{B_d}, B_{B_s}, B_{B_s}/B_{B_d}$, and B_K and the CKM parameters $|V_{ub}|$ and $|V_{cb}|$ by scanning over the range in the theory uncertainties using fixed grids or Monte Carlo (MC) methods. In the baseline fit, we combine measurements of $\Delta m_d, \Delta m_s, \varepsilon_K, |V_{cb}|, |V_{ub}|, |V_{ud}|, |V_{us}|, \sin 2\beta, \alpha$ and γ in the χ^2 function:

$$\chi^2(\bar{\rho}, \bar{\eta}, p_i, t_j) = \left(\frac{\langle \Delta m_{d,s} \rangle - \Delta m_{d,s}(\bar{\rho}, \bar{\eta}, p_i, t_j)}{\sigma_{\Delta m_{d,s}}} \right)^2 + \left(\frac{\langle |V_{cb,ub,ud,us}| \rangle - V_{cb,ub,ud,us}(\bar{\rho}, \bar{\eta}, p_i, t_j)}{\sigma_{V_{cb,ub,ud,us}}} \right)^2$$

$$+ \left(\frac{\langle |\varepsilon_K| \rangle - \varepsilon_K(\bar{\rho}, \bar{\eta}, p_i, t_j)}{\sigma_{\varepsilon_K}} \right)^2 + \left(\frac{\langle S_{\psi K^0} \rangle - \sin 2\beta(\bar{\rho}, \bar{\eta}, p_i)}{\sigma_{S_{\psi K^0}}} \right)^2 + \left(\frac{\langle \alpha \rangle - \alpha(\bar{\rho}, \bar{\eta}, p_i)}{\sigma_\alpha} \right)^2$$

$$+ \left(\frac{\langle \gamma \rangle - \gamma(\bar{\rho}, \bar{\eta}, p_i)}{\sigma_\gamma} \right)^2 + \sum_k \left(\frac{\langle \mathcal{M}_k \rangle - \mathcal{M}_k(p_i)}{\sigma_{\mathcal{M}_k}} \right)^2 + \sum_n \left(\frac{\langle \mathcal{T}_n \rangle - \mathcal{T}_n(p_i, t_j)}{\sigma_{\mathcal{T}_n}} \right)^2, \qquad (2.1)$$

where the p_i are measured quantities including the Wolfenstein parameters A and λ and the t_j are QCD parameters. The latter have theory errors that we scan over and "statistical" uncertainties we account for by including terms in the χ^2 in which the central values are taken from the lattice calculations. These are denoted by $\mathcal{T}_n$. To account for correlations in different observables such as quark and *B* meson masses, we add terms in the χ^2 denoted by $\mathcal{M}_k$. Table 1 lists the input values for our baseline fits and table 2 summarizes the QCD parameters. We presently do not scan the parameters $\eta_{cc}, \eta_{tc}, \eta_{tt}$ and η_b also listed in table 2, but we parametrize η_{cc} and its uncertainty in terms of m_c and α_s. For each choice of a set of theory parameters we determine the χ^2. For fits with a probability of $P(\chi^2) > 5\%(32\%)$, we plot 95% (68%) confidence level (CL) $\bar{\rho} - \bar{\eta}$ contours and study correlations among the theory parameters. The contours of all accepted fits are overlaid. We then use the extrema of this set of contours to determine an allowed range of $\bar{\rho}$ and $\bar{\eta}$ for a given confidence interval with no assumption as to the distribution of theoretical errors.

3. Comparison with CKMfitter and UTfit

First, we compare the performance of the scan method with that of CKMfitter [3] and UTfit [4] using 19 input measurements ($|V_{ud}|, |V_{us}|, |V_{cb}|, |V_{ub}|, \varepsilon_K, \Delta m_d, \Delta m_s, \sin 2\beta, \alpha, \gamma, f_{B_s}, B_{B_s}, f_{B_s}/f_{B_d}, B_{B_s}/B_{b_d}, B_K, m_t, mc, m_{B_d}, m_{B_s}$)[1] specified for the *B* Factory Physics Book [5] to fit 13 parameters ($\bar{\rho}, \bar{\eta}, A, \lambda, f_{B_s}, B_{B_s}, f_{B_s}/f_{B_d}, B_{B_s}/B_{b_d}, B_K, m_t, m_c, m_{B_d}, m_{B_s}$). For fits with a probability $P(\chi^2) > 32\%$, we plot 1σ contours in the $\bar{\rho} - \bar{\eta}$ plane. For the central value, we select the fit with the

---

[1]For α and γ, we presently use central values and measurement errors in the χ^2 function.

Table 1: Observables used in the baseline fits. The first (second) set of $|V_{cb}|$ and $|V_{ub}|$ values are the inputs used in the physics book of the B factories (from PDG12 with separate experimental and theory uncertainties).

m_t [GeV/c^2]	m_c [GeV/c^2]	Δm_d [ps^{-1}]	Δm_s [ps^{-1}]
173.5 ± 0.9	1.275 ± 0.025	0.507 ± 0.004	17.7 ± 0.08
$|V_{cb}|$	$|V_{ub}|$	$|V_{ud}|$	$|V_{us}|$
$(4.06 \pm 0.13) \times 10^{-2}$	$(3.89 \pm 0.44) \times 10^{-3}$	0.97427 ± 0.00021	0.2254 ± 0.0009
$(4.09 \pm 0.06 \pm 0.11) \times 10^{-2}$	$(4.15 \pm 0.1 \pm 0.48) \times 10^{-3}$		
ε_K	$\sin 2\beta$	α	γ
$(2.228 \pm 0.0011) \times 10^{-3}$	0.0676 ± 0.02	$(90 \pm 5)^o$	$(76 \pm 10)^o$

highest $P(\chi^2)$. We take the $\pm 1\sigma$ uncertainties from the maximum and minimum values of the envelope of all contours. We perform three different types of fits. In type I fits, we combine theory and experimental uncertainties and treat these as Gaussian. In type II fits, we scan over the theory uncertainties in $f_{B_s}, f_{B_s}/f_{B_d}, B_K$. In type III fits, we extend our scans over the theory uncertainties in $|V_{ub}|$ and $|V_{cb}|$ using PDG averages [6] in which we separated experimental and theory uncertainties. Note that the PDG applies scaling factors of 2.6 and 2.0 for the uncertainties in $|V_{ub}|$ and $|V_{cb}|$, respectively since esults from exclusive modes are significantly lower than those from inclusive modes.

Figure 1 (left) shows the overlay of 1σ contours in the $\bar{\rho} - \bar{\eta}$ plane for accepted type II fits and Fig. 1 (right) shows those those for type III fits. Table 3 lists our results in comparison to those from CKMfitter and UTfit. All three methods yield similar results. Without scanning, the uncertainties in the unitarity triangle parameters are smaller than those from CKMfitter and UTfit. When scanning theory uncertainties of QCD parameters only, the allowed region in the $\rho - \bar{\eta}$ plane increases significantly. When scanning in addition the theory uncertainties in $|V_{ub}|$ and $|V_{cb}|$, the allowed region increases by more than a factor of two. Note that we presently scan exactly the range of uncertainty given by the theorists. However, this may not be sufficient and the ranges may need to be increased. In all subsequent global fits of the CKM matrix, we scan over theory uncertainties in $|V_{ub}|, |V_{cb}|, f_{B_s}, f_{B_s}/f_{B_d}$ and B_K.
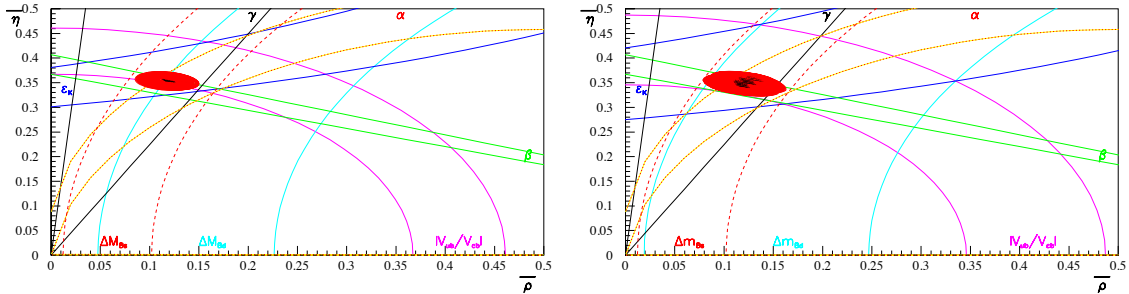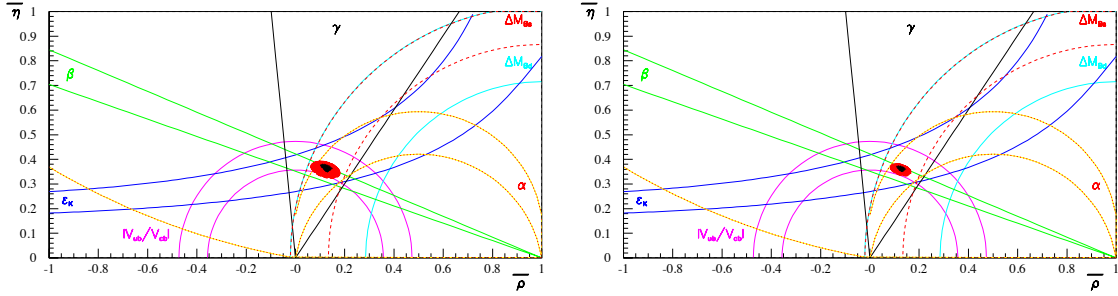

Figure 1: Overlay of 68% CL contours in the $\bar{\rho} - \bar{\eta}$ plane for the inputs of the physics book of the B factories with scanning over $f_{B_s}, f_{B_s}/f_{B_d}, B_K$ (left) and additional scanning over $|V_{ub}|$ and $|V_{cb}|$ (right).

Table 2: QCD parameters used in the baseline fits with "statistical" and theory uncertainties, respectively.

f_{B_s} [MeV]	f_{B_s}/f_{B_d}	B_{B_s}	B_{B_s}/B_{B_d}	B_K
$250 \pm 5.4 \pm 11$	$1.215 \pm 0.012 \pm 0.015$	1.33 ± 0.06	1.05 ± 0.06	$0.737 \pm 0.006 \pm 0.020$

η_{cc}	η_{tc}	η_{tt}	η_b	
1.39 ± 0.35	0.47 ± 0.04	0.5765 ± 0.0065	0.551 ± 0.007	

Table 3: Comparison of unitarity triangle parameters for different fitting techniques using inputs for physics book of the B-factories. The second column shows fit results if no scanning over theory parameters is performed. The third (fourth) column shows fit results if we scan over the QCD parameters $f_{B_s}, f_{B_s}/f_{B_d}, B_K$ (and over $|V_{ub}|$ and $|V_{cb}|$). The fifth and sixth columns show results from CKMfitter and UTfit.

Parameter	Type I fit	Scan method, type II fit	Scan method, type III fit	CKMfitter	UTfit
	no scan	scan over $f_{B_s}, f_{B_s}/f_{B_d}, B_K$	scan in addition $|V_{cb}|$ and $|V_{ub}|$		
$\bar{\rho}$	0.119 ± 0.013	$0.116^{+0.034}_{-0.031}$	$0.130^{+0.030}_{-0.051}$	0.121 ± 0.02	0.125 ± 0.022
$\bar{\eta}$	0.353 ± 0.008	$0.353^{+0.020}_{-0.018}$	$0.355^{+0.018}_{-0.032}$	0.349 ± 0.012	0.347 ± 0.014
$\beta \, [^o]$	21.9 ± 0.3	$21.8^{+0.9}_{-0.9}$	$22.2^{+0.4}_{-1.6}$	21.7 ± 1	21.6 ± 0.8
$\alpha \, [^o]$	86.8 ± 2	$86.4^{+5.1}_{-4.6}$	$87.9^{+6.3}_{-5.3}$	87.5 ± 3.2	87.9 ± 3.4
$\gamma \, [^o]$	71.4 ± 2	$71.8^{+4.8}_{-5.1}$	$69.8^{+7.4}_{-5.6}$	70.9 ± 3.2	70.4 ± 3.4

Figure 2: Overlay of 95% CL contours in the $\bar{\rho} - \bar{\eta}$ plane for the baseline fits with 19 measurements without $\mathscr{B}(B^+ \to \tau^+ \nu)$ (left) and with $\mathscr{B}(B^+ \to \tau^+ \nu)$ (right).

Table 4: The 95% CL ranges for unitarity triangle parameters from our baseline fits without and with $\mathscr{B}(B^+ \to \tau^+ \nu)$.
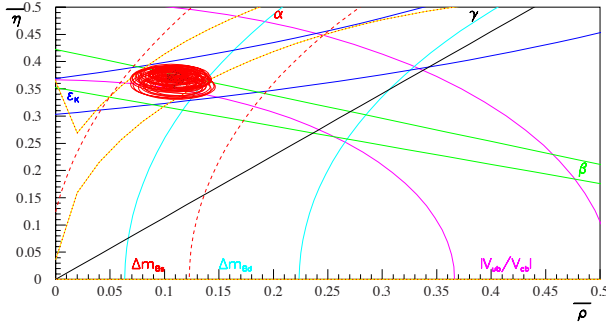
Parameter	$\bar{\rho}$	$\bar{\eta}$	$\beta \, [^o]$	$\alpha \, [^o]$	$\gamma \, [^o]$
Scan without $B \to \tau\nu$	$0.058 - 0.181$	$0.324 - 0.394$	$20.8 - 23.7$	$77.1 - 95.9$	$62.3 - 81.0$
Scan with $B \to \tau\nu$	$0.085 - 0.159$	$0.334 - 0.377$	$21.2 - 22.9$	$76.9 - 92.9$	$65.2 - 76.9$

4. Fit Results

To test the SM, we increase the requirement for accepted fits to $P(\chi^2) > 5\%$. Figure 2 (left) shows the overlay of 95% (CL) contours in the $\bar{\rho} - \bar{\eta}$ plane for all accepted baseline fits using 19 measurements to fit 13 parameters. Table 4 shows the 95% CL range of the unitarity triangle parameters. The $B^+ \to \tau^+ \nu$ branching fraction[2], measured by *BABAR* [7] and Belle [8] in different analyses, is very sensitive to contributions from a charged Higgs boson. The world average of $\mathscr{B}(B^+ \to \tau^+ \nu) = (1.66 \pm 0.33) \times 10^{-4}$ [10] is larger than the SM prediction of $\mathscr{B}(B^+ \to \tau^+ \nu) =$
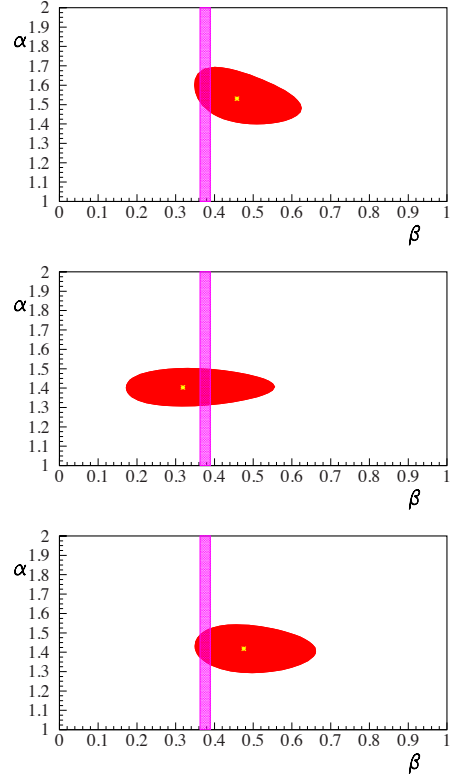
---

[2] *CP* conjugate states are implied

$(1.2 \pm 0.25) \times 10^{-4}$ [9]. CKMfitter [3] and UTfit [4] reported a conflict with the $\sin 2\beta$ measurement. Thus, we performed baseline fits in which we added $\mathcal{B}(B \to \tau^+\nu)$. Figure 2 (right) shows the results in the $\bar{\rho} - \bar{\eta}$ plane and Table 4 summarizes the 95% CL ranges of unitarity parameters. Even with the high values of $\mathcal{B}(B^+ \to \tau^+\nu)$, we obtain quite a sizable allowed $\bar{\rho} - \bar{\eta}$ region. At this conference, Belle presented a new result of $\mathcal{B}(B^+ \to \tau^+\nu) = (0.72^{+0.27}_{-0.25}{}_{stat} \pm 0.11_{sys}) \times 10^{-4}$ [11] which reduces the world average to $(1.14 \pm 0.23) \times 10^{-4}$ and in turn reduces the conflict in the SM with the other measurements of the unitarity triangle.

Figure 3: Overlay of 95% CL contours in the $\bar{\rho} - \bar{\eta}$ plane for fits with 230 measurements without $\mathcal{B}(B \to \tau^+\nu)$.

We also perform fits in which we replace α and γ by measurements that determine them. Omitting $\mathcal{B}(B^+ \to \tau^+\nu)$, this increases the number of measurements (parameters) in the fit to 230 (104). As replacement for α, we include all measured branching fractions and CP asymmetries in $B \to PP, PV, VV$ modes. The $B \to Pa_1$ modes are not yet included. Following the Gronau-Rosner approach [12], we parametrize amplitudes in terms of tree, color-suppressed tree, penguin, singlet penguin, W-annihilation/W-exchange, electroweak and color-suppressed electroweak diagrams (up to λ^2 beyond leading order). As a replace-

Figure 4: Contours at 95% CL in the $\alpha - \beta$ plane for $B \to PP$, $B \to PV$ and $B \to VV$ modes.

ment for γ, we use decay ratios and CP asymmetries of $B^+ \to D^{(*)}K^+$ and $B^+ \to DK^{*+}$ decays analyzed in the Giri-Grossman-Soffer-Zupan [13], Gronau-London-Wyler [14] and Atwood-Dunietz-Soni (ADS) methods [15]. We also include decay ratios and CP asymmetries of $B^+ \to D^{(*)}\pi^+$ decays analyzed in the ADS method and time-dependent CP asymmetries in $B^0 \to D^{(*)+}\pi^-$ and $B^0 \to D^{(*)+}\rho^-$ decays that determine $\sin(2\beta + \gamma)$. This procedure accounts for possible correlations between α, γ and the other Wolfenstein parameters (e.g. β). Figure 3 shows the 95% CL contours of all accepted fits in the $\bar{\rho} - \bar{\eta}$. The allowed region is smaller than that for the baseline fits. This is caused by the observation that $B \to PP$, VV ($B \to PV$) modes yield larger (smaller) values of β than the $\sin 2\beta$ measurement in $b \to c\bar{c}s$ decays (see table 5).

5. Determination of α

We also perform fits of the branching fractions and *CP* asymmetries in $B \to PP$, $B \to PV$ and $B \to VV$ modes separately to extract α. For each decay class, we plot $\alpha - \beta$ contours at 95% CL shown in Fig. 4. Table 5 shows the results of the fit for each decay class. The contours are rather wide and include the world average $\bar{\beta} = (21.4 \pm 0.8)^o$ measured in $b \to c\bar{c}s$ modes.

6. Conclusion

The three fitting methods yield similar results. By scanning over theory uncertainties in the QCD parameters (and $|V_{ub}|$ and $|V_{cb}|$), however, the allowed region in $\bar{\rho} - \bar{\eta}$ plane becomes significantly larger. Even for $\mathscr{B}(B^+ \to \tau^+ \nu) = (1.66 \pm 0.33) \times 10^{-4}$, we find global

Table 5: Measurements of α from fits of branching fractions and *CP* asymmetries in $B \to PP$, $B \to PV$ and $B \to VV$ decays.

Mode	α [^{o}]	β [^{o}]
$B \to PP$	86.5 ± 3.4	$25.8^{+4.0}_{-3.4}$
$B \to PV$	80.8 ± 4.0	$18.3^{+3.4}_{-2.9}$
$B \to VV$	81.4 ± 5.2	$27.5^{+7.4}_{-5.7}$

fits consistent with the SM at 95% CL. Using all measured branching fraction and *CP* asymmetries of $B \to PP$, $B \to PV$, $B \to VV$ modes and $B^+ \to D^{(*)}K^+$, $B \to DK^{*+}$ modes that respectively yield α and γ, we see a reduced allowed region in the $\bar{\rho} - \bar{\eta}$ plane. From separate fits of branching fractions and *CP* asymmetries in these modes, we determine $\alpha - \beta$ contours. Though α measurements agree with each other and β results are consistent with $\sin 2\beta$ measured in $b \to c\bar{c}s$ modes, the correlations among Wolfenstein parameters in the different measurements seem to be important.

References

[1] N. Cabibbo, Phys. Rev. Lett. **10**, 531 (1963); M. Kobayashi and T. Maskawa, Prog. Th. Phys. **49**, 652 (1973).

[2] G.P. Dubois-Felsmann *et al.*, arXiv:hep-ph/0308262v2 (2003).

[3] J. Charles *et al.*, Eur. Phys. Jour. **C41**, 1 (2005); updates at http://ckmfitter.in2p3.fr/.

[4] M. Bona *et al.*, JHEP **803**, 049 (2008); updates at http://www.utfit.org/.

[5] Physics Book of the *B* Factories, Eds. A. Bevan *et al.*, to be published, Springer Verlag (2013).

[6] J. Beringer *et al.* (Particle Data Group), Phys.Rev. **D86**, 010001 (2012).

[7] P. del Amo Sanchez *et al.*, Phys. Rev. **D81**, 051101 (2010); J.P. Lees *et al.*, arXiv:1207.0698 (2012).

[8] K. Hara *et al.*, Phys. Rev. **D.82**, 071101 (2010).

[9] D. Silverman and H. Yao, Phys Rev. **D38**, 214 (1998).

[10] D. Asner *et al.*, arXiv:1010.1589v3 (2011); www.slac.stanford.edu/xorg/hfag/triangle/index.html

[11] I. Adachi *et al.*, arXiv:1208.4678 (2012).

[12] M. Gronau *et al.*, Phys. Rev. **D50**, 4520 (1994); Phys. Rev. **D60**, 034021 (1999); ibid. **D69**, 119901 (2004); A.S. Dighe *et al.*, Phys. Rev. **D57**, 1783 (1998); M. Gronau and J. L. Rosner, Phys. Rev. **D61**, 073008 (2000); Phys. Rev. **D62**, 014031 (2000); A. Beneke *et al.*, Phys. Lett. **B638**, 68 (2006).

[13] A. Giri *et al.*, Phys. Rev. **D68**, 054018 (2003).

[14] M. Gronau and D. London, Phys. Lett. **B253**, 483 (1991); M. Gronau and D.Wyler, Phys. Lett. **B265**, 172 (1991).

[15] D. Atwood, I. Dunietz, A. Soni, Phys. Rev. Lett. **78**, 3257 (1997); Phys. Rev. **D63**, 036005 (2001).